Temporal dynamics of Copper-Based Nanopesticide transfer and subsequent modulation of the interplay between host and microbiota across trophic levels

Yan, X.; White, J.C.; He, E.; Peijnenburg, W.J.G.M.; Zhang, P.; Qiu, H.

ACSNANO

www.acsnano.org

ARTICLE

Temporal Dynamics of Copper-Based Nanopesticide Transfer and Subsequent Modulation of the Interplay Between Host and Microbiota Across Trophic Levels

Xuchen Yan, Jason C. White, Erkai He, Willie J.G.M. Peijnenburg, Peng Zhang, and Hao Qiu*

Cite This: *ACS Nano* 2024, 18, 25552–25564

Read Online

ACCESS | Metrics & More | Article Recommendations | Supporting Information

ABSTRACT: During agricultural production, significant quantities of copper-based nanopesticides (CBNPs) may be released into terrestrial ecosystems through foliar spraying, thereby posing a potential risk of biological transmission via food chains. Consequently, we investigated the trophic transfer of two commonly available commercial CBNPs, Reap2000 (RP) and HolyCu (HC), in a plant-caterpillar terrestrial food chain and evaluated impacts on host microbiota. Upon foliar exposure (with 4 rounds of spraying, totaling 6.0 mg CBNPs per plant), leaf Cu accumulation levels were 726 ± 180 and 571 ± 121 mg kg^{-1} for RP and HC, respectively. HC exhibited less penetration through the cuticle compared to RP (RP: 55.5%; HC: 32.8%), possibly due to size exclusion limitations. While caterpillars accumulated higher amounts of RP, HC exhibited a slightly higher trophic transfer factor (TTF; RP: 0.69 ± 0.20; HC: 0.74 ± 0.17, $p > 0.05$) and was more likely to be transferred through the food chain. The application of RP promoted the dispersal of phyllosphere microbes and perturbed the original host intestinal microbiota, whereas the HC group was largely host-modulated (control: 65%; RP: 94%; HC: 34%). Integrating multiomics analyses and modeling approaches, we elucidated two pathways by which plants exert bottom-up control over caterpillar health. Beyond the direct transmission of phyllosphere microbes, the leaf microbiome recruited upon exposure to CBNPs further influenced the ingestion behavior and intestinal microbiota of caterpillars via altered leaf metabolites. Elevated *Proteobacteria* abundance benefited caterpillar growth with RP, while the reduction of *Proteobacteria* with HC increased the risk of lipid metabolism issues and gut disease. The recruited *Bacteroidota* in the RP phyllosphere proliferated more extensively into the caterpillar gut to enhance stress resistance. Overall, the gut microbes reshaped in RP caterpillars exerted a strong regulatory effect on host health. These findings expand our understanding of the dynamic transmission of host-microbiota interactions with foliar CBNPs exposure, and provide critical insight necessary to ensure the safety and sustainability of nanoenabled agricultural strategies.

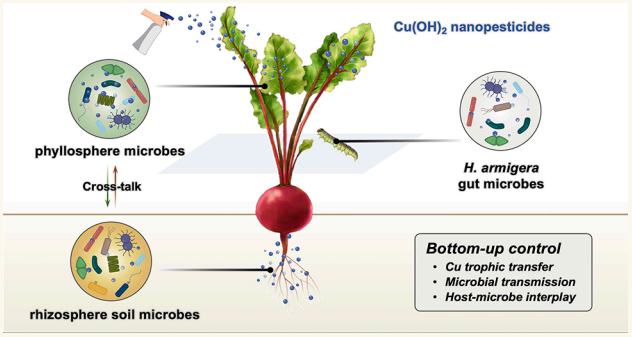

KEYWORDS: *nanopesticide, phyllosphere, host-microbiota, trophic transfer, ecotoxicology*

INTRODUCTION

In light of the challenges presented by a burgeoning global population and climate change, the inefficiency and lack of sustainability of traditional agriculture is highly concerning. Consequently, innovative crop management strategies utilizing nanotechnology have been developed to improve agricultural efficiency and productivity. With advancements in nanotechnology, copper-based nanopesticides (CBNPs) have emerged as more precise, effective, and environmentally friendly alternatives to conventional pesticides like the Bordeaux mixture [$CuSO_4$ + $Ca(OH)_2$], showcasing considerable potential for advancing sustainable agriculture.[1,2] Their specific physiochemical properties offer improved stability, controlled or even tunable release of active ingredients, lower applicate rates compared to traditional pesticides, and reduced

Received: May 7, 2024
Revised: August 13, 2024
Accepted: August 13, 2024
Published: August 22, 2024

https://doi.org/10.1021/acsnano.4c06047
ACS Nano 2024, 18, 25552–25564

environmental residues.[3] The widespread use of CBNPs in agriculture will introduce these compounds into terrestrial ecosystems, where they may impact material cycling and energy flow processes, potentially posing risks to environmental and human health. Therefore, it is imperative to conduct a thorough assessment of their environmental fate and potential impacts on edible plants and food chains to ensure safety and sustainability.

The foliar application of CBNPs such as $Cu(OH)_2$ and CuO nanopesticides has been seeing increased use to enhance crop resistance and reduce crop loss associated with pests and diseases. Compared to soil-root application, foliar spraying is more efficient in delivering active ingredients with increased bioavailability, resulting in a significant reduction of environmental losses.[4] Once sprayed, a substantial amount of nanopesticides can be captured by the leaves and then internalized through stomata, aqueous pores, and cuticle pathways.[4,5] Previous studies have shown that internalized CuO and SiO_2 nanoparticles typically distribute within the extracellular space of spongy mesophyll cells or cuticle layers;[6,7] importantly, the mechanisms by which irregularly shaped nanomaterials (e.g., nanorods and nanosheets) enter leaves and distribute across different tissue fractions remain poorly understood. However, it is clear that nanoscale morphology can influence the distribution of nanopesticides within leaves by directly modulating the epidermal penetration and interactions with the leaf surface,[6] consequently affecting analyte translocation.[8] Understanding these processes will provide valuable insights into the fate of CBNPs in plants and enable the optimization of overall efficacy.

CBNPs accumulated in leaves can be ingested by higher trophic-level invertebrate species such as caterpillars, introducing these analytes into the food chain and posing risks to additional biota within the food web.[9] Numerous studies have documented the trophic transfer of metal-based nanomaterials along the terrestrial food chain.[10,11] Although CBNPs may be applied to the aerial parts of plants in a fashion so as to minimize phytotoxicity, there is still a risk of copper contamination of food chains that rely on these plants as their primary producers.[12] In addition, the foraging habits of caterpillars vary during different developmental stages and these behavioral nuances can further impact toxicokinetic processes (uptake, distribution, metabolism, and elimination) of xenobiotics assimilated during food chain transfer. These dynamic processes directly affect the cumulative balance of contaminants and consequently influence their transfer efficiency across the entire food chain.[13] It is therefore crucial to develop an efficient kinetic model based on the concept of toxicokinetics (TK) to assess the dynamic CBNPs accumulation patterns in caterpillars at various developmental stages so as to clarify the underlying mechanism behind trophic transfer along the food chain.

Importantly, the significance of host microbiota has largely been ignored when assessing the fate and effects of toxicants in terrestrial food chains.[14,15] In fact, host microbiomes within food chains are known to be crucial for host adaptation to pollution stress, health, and overall trophic stability.[16] A number of studies have demonstrated the response mechanisms of plant-associated microbiomes upon nanomaterial exposure, as well as their role in regulating plant nutrient uptake, growth, and development.[16−18] However, these studies primarily focus on the interactions between plants and rhizosphere microorganisms rather than interactions between plants and above-ground tissue communities.[19,20] The phyllosphere provides a habitable niche for microbial colonization due to the large surface area, most of which is leaves.[21] Plants are known to both actively and passively biochemically recruit specific microbes and cultivate a dynamic phyllosphere community.[22] Phyllosphere microbes can maintain host fitness by inducing physiological changes in plants, producing antimicrobial substances, and competing with pathogens for ecological niches and nutrients, all while driving critical biogeochemical cycles within terrestrial ecosystems.[23−25] Phyllosphere microbes may potentially shift to soil through gas convection movement or plant activity, and may also be transferred to the intestines of herbivores by ingestion.[26] More importantly, microbes carried by plants (such as phyllosphere microbes) can cause potential downstream consequences in the guts of higher-trophic organisms, including reshaping the structure and diversity of the gut microbial community.[27−29] Intestinal microbes play a crucial role in maintaining animal host health by participating in various physiological processes such as food intake, energy metabolism, and immune regulation.[30] There is, however, a lack of information regarding the interplay of host and associated microbiota during contaminant trophic transfer processes. Given the increasing use of CBNPs, understanding the nanopesticide-mediated microbial transmission across trophic levels and the potential physiological mechanisms underlying bottom-up regulation of herbivores by plants is a topic in need of significant study.

The current study simulated a foliar exposure scenario and examined the Cu body burden and transfer of two commonly used commercial CBNPs, Reap2000, and HolyCu, in a cherry radish-caterpillar food chain. The impact on host microbiota across multiple trophic levels was determined, with a focus on modulation effects on host health. Our overall hypothesis is that an altered dietary composition as caused by CBNP application may influence the herbivore gut microbiome, leading to potentially cascading effects on their health. The objectives of this research are (1) to investigate the foliar uptake, translocation, and dynamic trophic transfer of two CBNPs in a model terrestrial food chain; (2) to elucidate the dispersal mechanisms and potential interspecific transmission of phyllosphere microbes along the food chain; (3) to construct a holistic framework illustrating the modulation effects of CBNPs on host-microbiota interactions across trophic levels. This study provides a comprehensive understanding of the food chain transfer risks associated with foliar spraying of CBNPs and offers a scientific basis for accurately evaluating their impact on agroecological system health.

RESULTS AND DISCUSSION

Characterization of CBNPs. RP and HC are rough rod-like structures with 146 ± 49 nm and 226 ± 98 in length, 38 ± 11 and 13 ± 2 nm in diameter, respectively (Figure S1). In deionized water, the hydrodynamic size of RP was approximately 241 ± 16 nm, whereas HC agglomerates to 2800 ± 331 nm. The polydispersity indices of RP and HC were 0.166 (<0.2) and 0.546 (>0.2), respectively, and the ζ potential values were −5.42 ± 0.64 mV for RP and −2.35 ± 0.30 mV for HC (Figure S2). The dissolution profiles after 7 days show 9.6% of Cu release from HC, whereas only 2.6% was released from RP (Figure S2a). CBNPs exhibited a higher potential for ion release in simulated xylem (∼30%) and phloem sap (∼50%), particularly in the case of HC (Figure S2b−c). Differences in particle size, dispersibility, and transformation

https://doi.org/10.1021/acsnano.4c06047
ACS Nano 2024, 18, 25552−25564

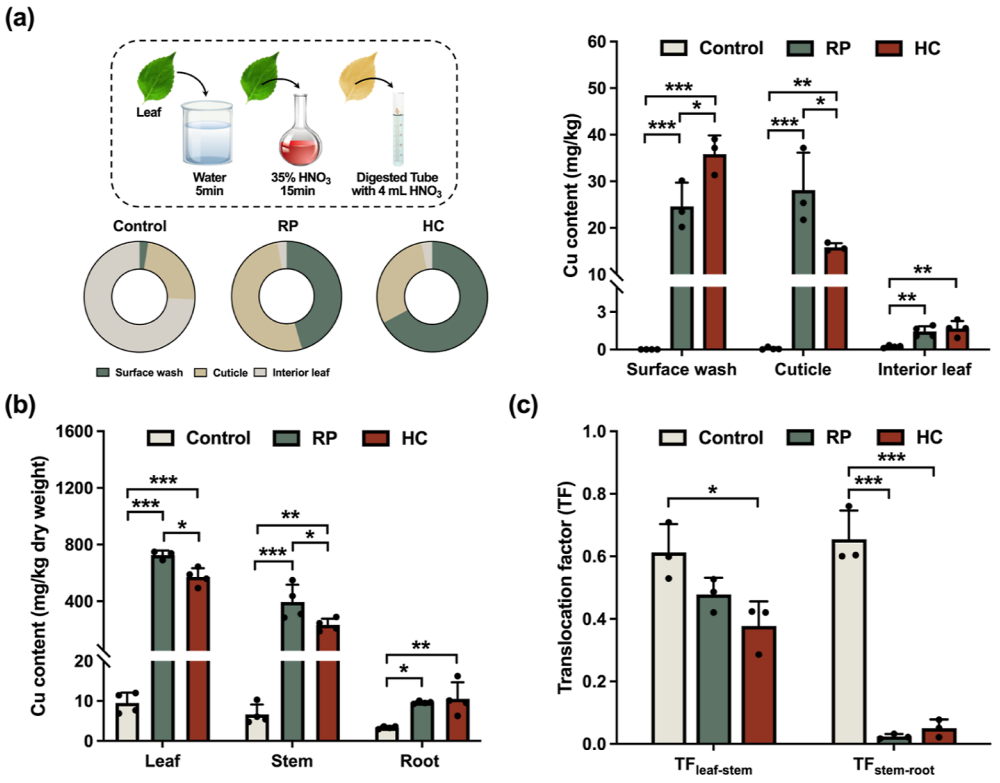

Figure 1. Effect of the $Cu(OH)_2$ nanopesticide foliar application on Cu uptake, accumulation, and translocation in cherry radish. The procedure for Cu extraction from the cuticle, and Cu contents in the surface wash, cuticle, and interior leaves of cherry radish leaves (a); Cu concentrations in leaves, stems, and roots of cherry radish (b), and translocation factors of Cu in the different treatments (c). [Note: data are expressed as mean ± SD (standard deviation); statistically significant differences between treatments are indicated by * ($p < 0.05$), ** ($p < 0.01$), and * ($p < 0.001$); the Cu concentration in leaves is defined as the sum of Cu content in cuticle and interior leaf].**

potential between the two CBNPs may impact in planta particle fate, thereby influencing subsequent trophic transfer.

Physiological and Biochemical Responses of Cherry Radish. The biomass of cherry radish shoots and roots significantly increased with the foliar application of RP and HC, showing a 95 and 104% increase in shoots and a 297 and 61% increase in roots compared to controls (Figure S3a). These results are likely due to enhanced photosynthetic activity in CBNP-treated plants, as indicated by a significant increase of 35−47% in chlorophyll content (Figure S3c). CBNPs can stimulate the production of cytokinins, promoting metabolic activity and cell growth, thereby enhancing chlorophyll levels.[31] Alternatively, they can directly regulate chloroplast function and chlorophyll content through copper *P*-type ATPases or form complexes with pigments to stabilize chlorophyll.[32] Additionally, copper can participate in plant physiological processes, including enhancing plastocyanin activity in photosynthetic electron transfer, which is crucial for maintaining electron flow and optimizing photosynthetic efficiency.[33] Additionally, RP and HC treatments resulted in 1.36- and 1.64-fold higher flavonoid content compared to the control, respectively, demonstrating enhanced antioxidant capacity that could improve overall plant health (Figure S4). Furthermore, CBNPs improved the physical barrier function of plants by increasing leaf Si concentrations (control: 46.8 mg kg^{-1}; RP: 78.8 mg kg^{-1}; HC: 64.7 mg kg^{-1}); in addition, an elevation in Fe (1.56-fold), Mn (1.10-fold), and Al (1.48-fold) levels were observed in roots of HC-treated plants compared to controls (Figure S3d). This is possibly due to upregulated transporter gene expression for these elements.[34] These findings suggested that copper homeostasis may potentially regulate the uptake of other micro- and macro-elements, as well as overall crop nutritional quality, by altering primary leaf metabolism and gene expression.[35] Previous studies have demonstrated that engineered nanomaterials can regulate reactive oxygen species levels and the activities of stress-responsive enzymes in plants.[36,37] Here, superoxide dismutase activity was inhibited under RP and HC treatment (Figure S4); this could be attributed to the negative regulation of CBNPs and a lower $O_2^{\bullet-}$ concentration caused by the enhanced content of flavonoid scavenging free radicals.[38] Despite the initial inhibition of defense by CBNPs, the enhanced peroxidase activity bolstered the secondary defenses in plants, thereby minimizing oxidative damage to a certain extent. Plants may selectively trigger signaling pathways to induce the expression of antioxidant enzyme or secrete secondary metabolites, such as flavonoids, in order to regulate the activity of specific antioxidant enzymes under specific conditions, thereby achieving a more efficient oxidative−reductive balance.[39,40] Based on these findings, it is clear that CBNPs not only enhanced the nutritional status of cherry radish but also activated key defensive pathways. Notably, the enzymatic and nonenzymatic antioxidant defense systems synergistically operate to efficiently maintain overall plant homeostasis.

Plant Uptake and Accumulation of CBNPs. The leaves treated with RP and HC exhibited significant absorption of Cu, reaching levels of 726 ± 180 and 571 ± 121 mg kg^{-1}, respectively (Figure 1). In certain cases, smaller nanoparticles were found to be more efficiently taken up by the leaves

https://doi.org/10.1021/acsnano.4c06047
ACS Nano 2024, 18, 25552−25564

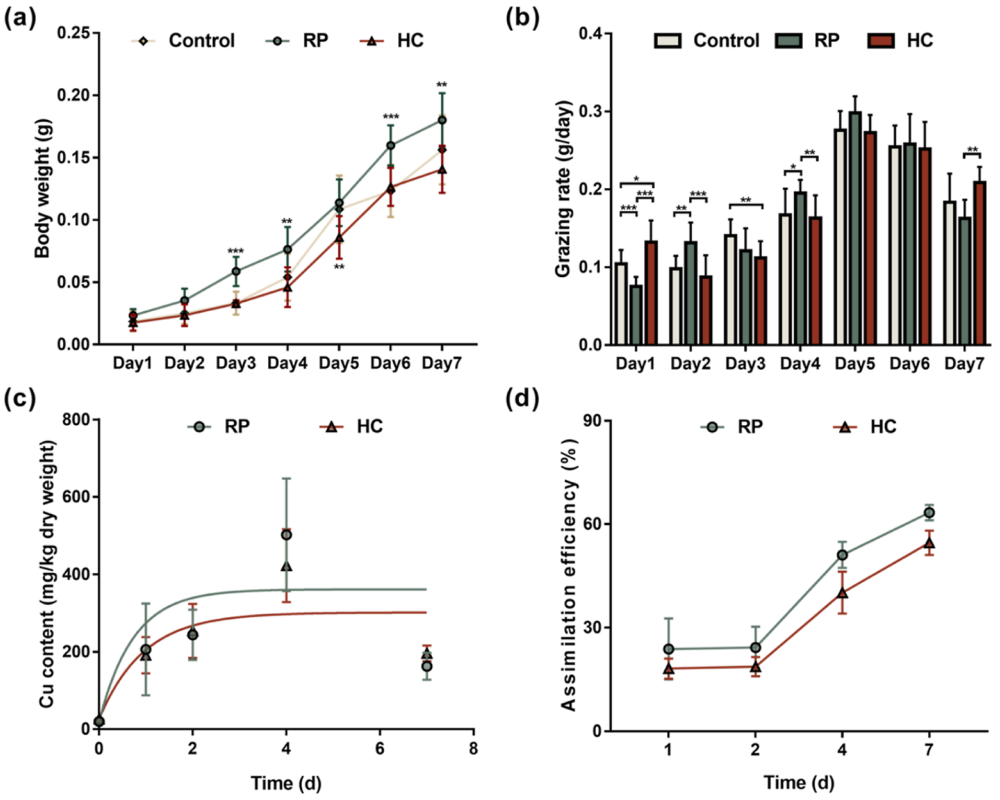

Figure 2. Effect of the $Cu(OH)_2$ nanopesticide foliar application on *H. armigera* caterpillars via trophic transfer. Body weight (a) and grazing rate (b) of *H. armigera* caterpillars during the exposure period; accumulation of $Cu(OH)_2$ nanopesticides in *H. armigera* caterpillars (c); and assimilation efficiency of *H. armigera* caterpillars exposed for 7 days (d). [Note: data are expressed as mean ± SD (standard deviation); statistically significant differences between treatments are indicated by * ($p < 0.05$), ** ($p < 0.01$), and * ($p < 0.001$). In (a), statistical analysis was solely conducted on the daily weight difference of *H. armigera* within each treatment group, without incorporating time factor].**

compared to larger counterparts due to size-dependent effects.[41] The presence of RP facilitated Cu accumulation within plant leaves with a higher bioaccumulation factor (BAF) (RP: 1.13 ± 0.13; HC: 0.81 ± 0.09; significantly different at $p < 0.05$), likely attributed to its lower degree of aggregation as indicated by hydrodynamic diameter and dispersibility data. Moreover, the Cu content in the surface wash fraction was 24.6 ± 5.1 and 35.9 ± 4.0 mg kg^{-1} (Significantly different at $p < 0.05$) in the RP and HC treatment, respectively. Foliar-applied HC had a significantly higher adhesion percentage and exhibited less penetration through the cuticle compared to an equivalent Cu dose of RP (RP: 55.5%; HC: 32.8%) (Figure 1). The results of a cuticle isolation experiment demonstrated distinct storage strategies between two types of CBNPs. The Cu accumulation in cuticle suggests that apart from using stomatal pathway, dissolution reactions initiated by weak acidic metabolites on leaf surfaces may serve as an alternate route for CBNP entry.[34] Dissolved Cu^{2+} can either permeate the epidermal cells or traverse the cuticle region upon momentary disruption of the cuticular layers.[42,43] Furthermore, NPs' surface chemistry determines their interaction with leaves and subsequently affects leaf uptake.[44,45] Once they cross through both the cuticle and epidermis, CBNPs can enter phloem via symplastic or apoplastic pathways with more ion release (Figure S2) before being transported to other plant organs from exposed leaves.[44] The Cu content in other cherry radish tissues also showed significant increases compared to controls (control: 6.65 ± 2.50 mg kg^{-1}, RP: 395 ± 122 mg kg^{-1}, HC: 233 ± 44 mg kg^{-1} in stems; control: 3.38 ± 0.33 mg kg^{-1}, RP: 9.64 ± 0.33 mg kg^{-1}, HC: 10.6 ± 4.1 mg kg^{-1} in roots). The significantly lower Cu content in the leaves of the HC group and comparable levels in the roots suggested higher interplant mobility than RP. However, there was no significant difference observed in the ability of Cu migration from leaves to stems or from stems to roots between the two treatment groups. The variation in CBNP translocation may be attributed to morphological transformations occurring during leaf uptake. Both CBNPs retained on the surfaces of leaves and those transported into the xylem exhibited a higher potential for ion release in HC, as evidenced by the observed Cu^{2+} release in dissolution experiments (Figure S2). Once inside the plant, CBNPs may develop coronas that further influence their transport dynamics; copper ions follow their typical distribution patterns, although additional investigation on this topic is warranted. Despite the observation of Cu translocation within the plant, the shoot-to-root translocation factor (TF, Cu in roots/Cu in leaves) was significantly lower (0.011−0.018) in CBNP-treated plants compared to controls (0.40). Similarly, Zhao et al.[1] demonstrated that CBNP translocation was obstructed in foliar-treated lettuce, with 97−99% of CBNPs remaining in the leaves. This could be attributed to size exclusion limits since current evidence suggests that only NPs smaller than cell wall pores (approximately 20 nm) can undergo phloem translocation from leaves.[44] Therefore, CBNPs transported to the stem and roots are likely to be present in the form of ions. RP and HC exhibit distinct accumulation and distribution patterns subject to hydraulic

https://doi.org/10.1021/acsnano.4c06047
ACS Nano 2024, 18, 25552−25564

properties and other factors, resulting in different impacts on the treated plants.

Dynamic Evaluation and Trophic Transfer of CBNPs. During the exposure period, caterpillar weight increased across all treatments at rates consistent with normal grazing (Figure 2a–b). After feeding on contaminated leaves for 7 days, the Cu content in the caterpillars reached apparent equilibrium, with levels of 502 ± 45.3 and 423 ± 34.5 mg kg^{-1} for RP and HC, respectively (Figure 2c), showing no significant difference ($p > 0.05$) between treatments. The bioaccumulation data for *Helicoverpa armigera* obtained over time fitted well with a one-compartment TK model. The uptake (K_u) and elimination rates (K_e) were calculated as 0.68/0.55 (g_{leaf} g*H. armigera*$^{-1}$ day^{-1}) and 1.36/1.05 (day^{-1}) for the RP/HC treatment groups, respectively (Table 1). The caterpillar K_u of Cu was higher for RP than compared to the HC treatment, as reflected by the slope of the Cu accumulation curves over time (Figure 2c), which could be related to the distinct physicochemical properties of the two CBNPs. Differences in the solubility of CBNPs within the exposure system resulted in differential toxicity, accumulation, and elimination kinetics among different forms of CBNP in caterpillars.[12] Although food ingestion rates were higher with HC, caterpillars fed RP-treated leaves exhibited greater assimilation efficiency (AE) and a lower mobility index (MI, Cu transport from body to feces), leading to higher Cu accumulation within their bodies (Figure S5). The higher values of K_u and AE for RP suggest greater bioavailability across trophic levels. This may be a function of CBNP transformation into ionic form during trophic processes. Different Cu forms have distinct transfer mechanisms in invertebrates; for example, the ion form has been shown to be readily assimilated and transported within herbivores through ion transport channels, in contrast to metal nanoparticles.[10] The study conducted by Morgado et al. (2022) also demonstrated that compared to CBNPs, traditional Cu^{2+} pesticides exhibited a higher tendency to accumulate in invertebrates, resulting in greater toxicity.[46] Importantly, the presence of herbivores significantly influences the fate of Cu from CBNPs, highlighting the complexity of biological ecosystems. After reaching equilibrium, trophic transfer factors across both treatments were lower than 1 (RP: 0.69 ± 0.20, HC: 0.74 ± 0.17, $p > 0.05$), suggesting that CBNPs are unlikely to biomagnify during trophic transfer. These trends support the concept of trophic dilution,[47] which can be explained by the relatively high values of MI in the RP and HC treatments, with values of 19.1 and 9.26, respectively.

Table 1. Overview of Toxicokinetic Parameters Estimated for *H. armigera* Exposed to Two Types of $Cu(OH)_2$ Nanopesticides (RP: Reap2000; HC: HolyCu) and Trophic Transfer Factors From Cherry Radish Leaves to *H. armigera*

treatment	K_u (g_{leaf} $g_{H.\ armigera}^{-1}$ day^{-1})[a]	K_e (day^{-1})	$t_{1/2}$	R^2	BAF	TTF
RP	0.68	1.36	0.51	0.53	1.13	0.69
HC	0.55	1.05	0.66	0.63	0.81	0.74

[a] K_u represents the uptake rate constant (g_{leaf} $g_{H.\ armigera}^{-1}$ day^{-1}); K_e represents the elimination rate constant (day^{-1}); $t_{1/2}$ represents the time needed to eliminate 50% of nanopesticides in *H. armigera* and is calculated from K_e; BAF represents bioaccumulation factor; TTF represents trophic transfer factor.

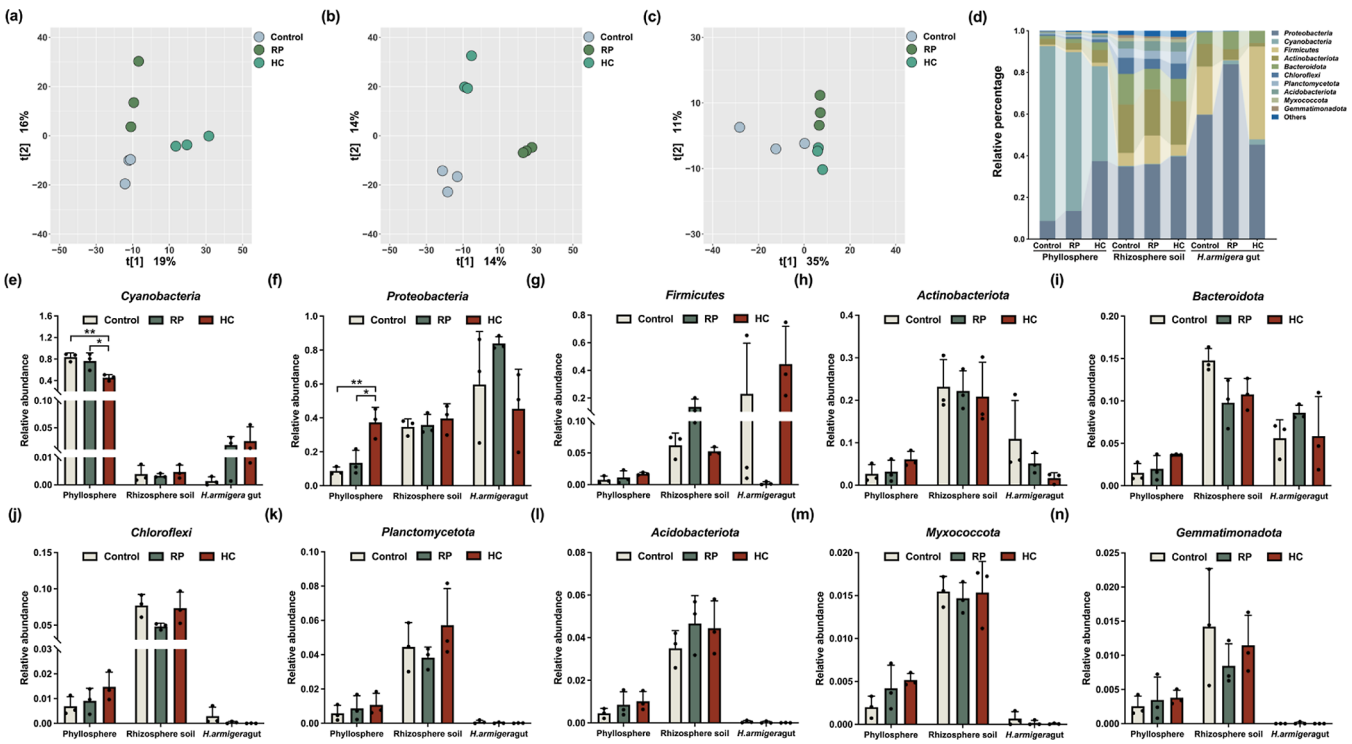

Figure 3. Effect of the $Cu(OH)_2$ nanopesticide foliar application on microbes in the phyllosphere, rhizosphere soil, and *H. armigera* gut. PLS-DA score plots of the bacterial community in (a) phyllosphere, (b) rhizosphere soil, and (c) *H. armigera* gut; composition of microbial indicator species in various biotopes (d); and relative abundance of the dominant bacterial at the level phyla (top 10) in phyllosphere, rhizosphere soil, and *H. armigera* gut (e–n). [Note: data are expressed as mean ± SD (standard deviation); statistically significant differences between treatments are indicated by * ($p < 0.05$), ** ($p < 0.01$), and * ($p < 0.001$)].**

https://doi.org/10.1021/acsnano.4c06047
ACS Nano 2024, 18, 25552–25564

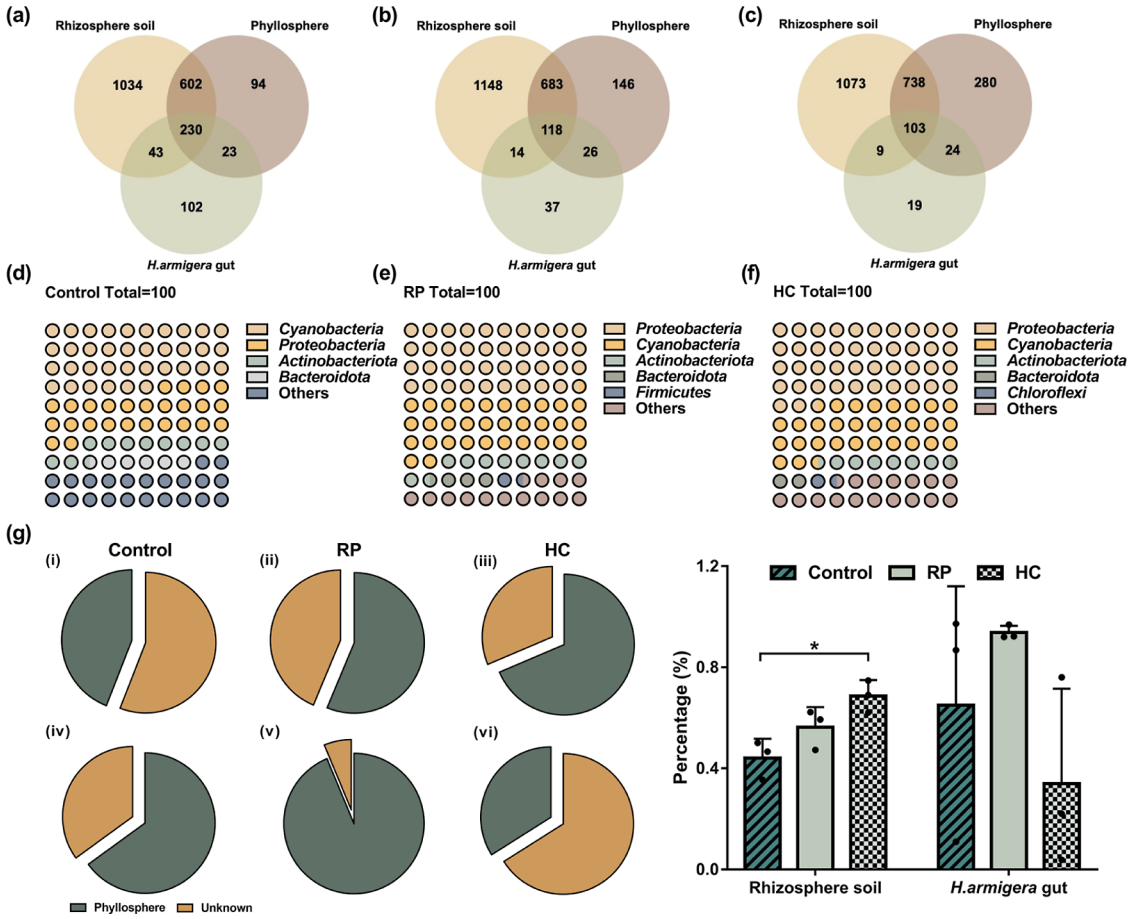

Figure 4. Edwards−Venn diagram of the shared OTUs in the phyllosphere, rhizosphere soil, and *H. armigera* gut for control (a), RP (b), and HC (c) treatments. Composition of OTUs common to different microhabitats in control (d), RP (e), and HC (f) treatments. Source tracking analysis to reveal the proportion of phyllosphere microbes attributed to the rhizosphere microbes (i−iii) and *H. armigera* gut microbes (iv−vi) for all treatments (g). [Note: data are expressed as mean ± SD (standard deviation); statistically significant differences between treatments are indicated by * ($p < 0.05$), ** ($p < 0.01$), and * ($p < 0.001$)].**

These findings suggest that CBNPs captured in higher-level consumers can be progressively eliminated through digestion and excretion processes. This aligns with previous studies where limited bioconcentration of TiO_2 nanoparticles was observed in larval growth experiments, with most of the burden being excreted rather than accumulated within the larvae's gut.[48,49] Overall, these results do demonstrate that foliar-applied CBNPs can cause Cu accumulation within leaves, with subsequent transfer from plants to herbivores through the food chain.

Compositional Structure and Microbial Shifts Across Phyllosphere-, Rhizosphere-, and *H. armigera* Gut-Associated Compartments. Partial least-squares discriminant analysis (PLS-DA) revealed a distinct separation of microbial communities associated with the phyllosphere as a function of treatment (Figure 3a). This shows that CBNPs induced overt changes in the phyllosphere microbial community composition. The first principal component explained 19% of the differences, with HC treatment being the most disparate. In the phyllosphere, the dominant phyla (relative abundance >40%) were *Cyanobacteria*, which decreased significantly with CBNP exposure. However, other phyla, particularly *Proteobacteria* (relative abundances: control: 8.69%, RP: 13.5%, HC: 36.4%) increased in relative abundance with treatments. *Proteobacteria* are commonly prevalent in the phyllosphere and are often associated with nutrient availability.[50] Previous studies have also suggested that *Proteobacteria* can inhibit other leaf endophytic bacteria through pattern-triggered immunity and the MIN7 vesicle-trafficking pathway.[30] The observed significant increase in *Proteobacteria* suggests a possible mechanism for the more evenly distribution of all species in HC-impacted phyllosphere microbes, as demonstrated by the significantly higher Shannon index, a comprehensive index used to evaluate the evenness and richness of microbial communities (Figure S6). The phyllosphere microbes in the HC treatment exhibited a greater capacity for adapting to environmental stress compared to RP, as evidenced by an increased Shannon and a decreased Simpson diversity index. Furthermore, it is notable that the use of CBNPs has the potential to enrich microorganisms that possess antistress response systems, i.e., *Proteobacteria* and *Firmicutes*. These species have been shown to survive and maintain active metabolism in adverse environments by participating in metal resistance and reduction, sulfide oxidation, nitrification, and ammonia oxidation reactions to reduce Cu bioavailability when present at excessive concentrations.[51] CBNPs application also effectively regulated the core microbial community in the phyllosphere and altered the network complexity with increased modularity values (Table S3). Interestingly, aggregation of sustained CBNPs on plant

https://doi.org/10.1021/acsnano.4c06047
ACS Nano 2024, 18, 25552−25564

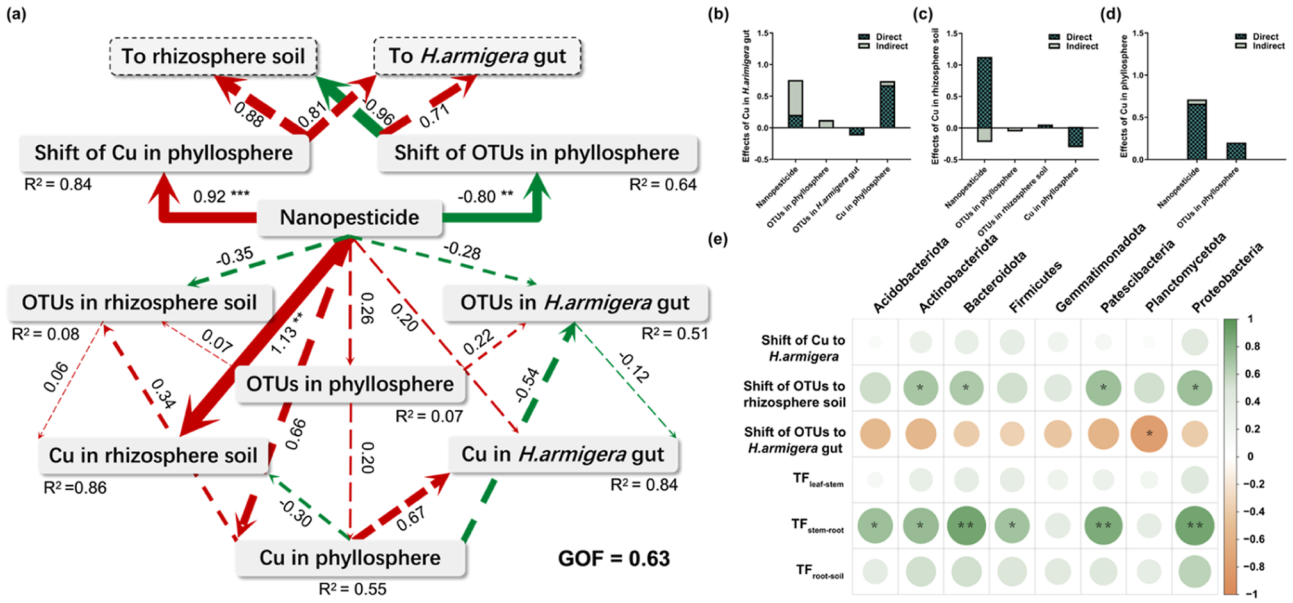

Figure 5. Path analysis results of the direct and indirect effects of nanopesticides, phyllosphere, rhizosphere soil, *H. armigera* gut OTUs; Cu in phyllosphere, rhizosphere soil, and *H. armigera* gut (a). Quantification results for the direct and indirect effects of Cu in *H. armigera* gut (b), rhizosphere soil (c), and phyllosphere (d). Correlation analysis reveals the microbial indicator species involved in the shift of copper and microbes (e). [Note: numbers show the standardized path coefficients. The arrow width is proportional to the standardized path coefficients. R^2 indicates the proportion of variance explained for each latent variable. GOF: the goodness of fit of the model. Solid and dashed arrows represent significant ($p < 0.05$) and nonsignificant ($p > 0.05$) paths, respectively. Significant levels are * ($p < 0.05$), ** ($p < 0.01$), and * ($p < 0.001$)].**

surfaces provides stable ecological niches for phyllosphere microbial interactions. This overall viewpoint is consistent with Shi et al.,[52] who reported that nanoplastics reinforce co-occurrence patterns of microbial communities dealing with external disturbances. In the present study, foliar CBNP application also indirectly influenced the soil by significantly impacting rhizosphere microbial communities (Figure 3b), despite a minimal amount of Cu leaching into the soil (below the soil screening value of 50 mg/kg). This indirect influence may be attributed to the migration of phyllosphere microbes recruited within plants through vascular systems.[21] Furthermore, CBNP-induced plant metabolism can lead to alterations in root exudates, ultimately affecting rhizosphere microbial community stability, as reflected by changes in Simpson diversity index in both treatments (Figure S6). Additionally, it is also possible that CBNP-treated plants exhibit copper exudation which subsequently affects rhizosphere microorganisms; this hypothesis finds support from previous findings demonstrating significant gold exudation resulting from foliar gold nanoparticle application.[43] The rhizosphere microbial community diversity of RP and HC-treated groups exhibited an opposite trend compared with the control group, which could be attributed to the differences in Cu exudation levels and root exudate composition. In addition, a divergence of gut microbial communities between groups with CNBPs was evident, although likely diluted after trophic transfer (Figure 3c). At the phylum level, both RP and HC exerted effects on the gut microbiota of caterpillars, primarily impacting *Proteobacteria*, *Firmicutes*, *Bacteroidota*, and *Actinobacteriota* ($p > 0.05$). Although no statistically significant differences were observed in the relative abundance of *Proteobacteria* (Figure 3), the observed reduction of *Proteobacteria* abundance in HC-treated caterpillars suggests a potential negative impact on lipid metabolism and gut health.[53] Additionally, *Bacteroidota* have been associated with abnormal intestinal permeability, while Actinobacteria may play a role in intestinal immunity and susceptibility to exogenous contaminants.[54] Collectively, these findings suggest that stressors at lower trophic levels may potentially influence the host-microbiota of higher trophic level species through food chain transfer processes.

On this basis, the transmission of host-microbiota during the process of CNBP trophic transfer was further explored. Venn diagrams reveal that the highest number of shared operational taxonomic units (OTUs) was observed in control samples (230, 10.8%), followed by RP (118, 5.4%), and HC (103, 4.6%) (Figure 4a–c). This result can be attributed to an increase in the distinctiveness of the phyllosphere OTUs (control: 4.4%, RP: 6.7%, HC: 12.5%) as a function of CBNP and its antimicrobial effects. The transmitted microbial community primarily comprised several taxa with relatively high abundance, including the phylum *Cyanobacteria*, *Proteobacteria*, *Actinobacteriota* and *Bacteroidota* (Figure 4d–f). These bacterial groups generally exhibited dominance in the phyllosphere. The dispersal and enrichment of *Firmicutes* in RP rhizosphere soil may have been driven by the response of the host plant to abiotic stress factors that contributed to improving host fitness via the modulation of soil nutrient cycling.[55,56] Additionally, the Bayesian SourceTracker algorithm was employed to evaluate the extent to which these microbiomes were derived from the phyllosphere microbes through host regulation and dietary intake. As depicted in Figure 4g, it was predicted that RP exposure facilitated the dispersal of microorganisms into rhizosphere soil (control: 44.1%; RP: 56.3%) and *H. armigera* gut (control: 65.0%; RP: 93.7%), with a higher proportion originating from phyllosphere microbes. The intestinal microbial community with RP suffered negative impacts due to mass colonization and assembly of phyllosphere microbes. This phenomenon became

https://doi.org/10.1021/acsnano.4c06047
ACS Nano 2024, 18, 25552–25564

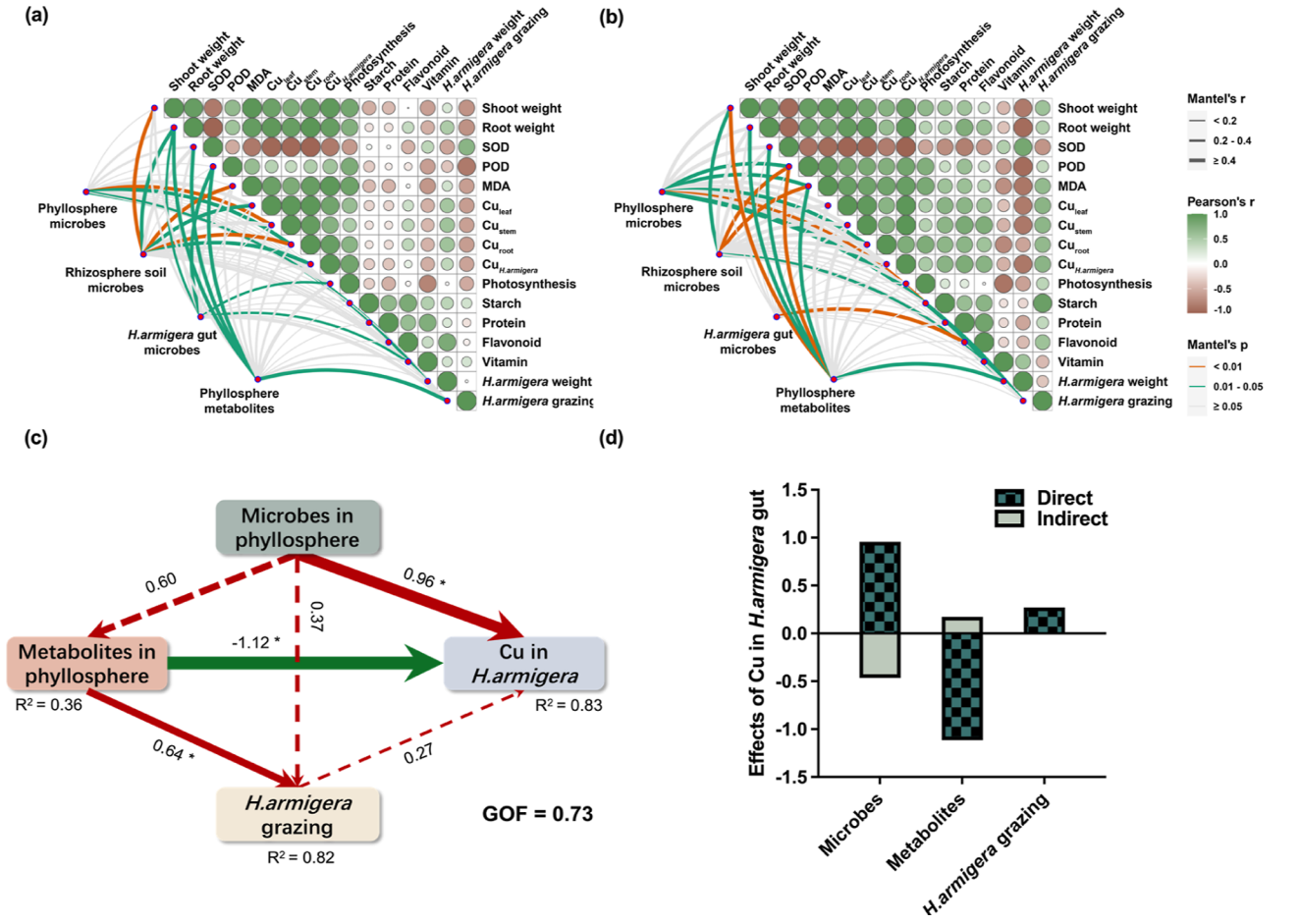

Figure 6. Mantel analysis examining the relationship between the physicochemical properties of cherry radish and *H. armigera*, the bacterial community structure, and metabolite profiles for RP (a) and HC (b) treatments. Path analysis results of the direct and indirect effects of microbes and metabolites in the phyllosphere, Cu content in *H. armigera* and *H. armigera* grazing (c), and the quantification results for the direct and indirect effects of Cu content in *H. armigera* (d). [Note: numbers show the standardized path coefficients. The arrow width is proportional to the standardized path coefficients. R^2 indicates the proportion of variance explained for each latent variable. GOF: the goodness of fit of the model. Solid and dashed arrows represent significant and nonsignificant ($p > 0.05$) paths, respectively. Significant levels are * ($p < 0.05$), ** ($p < 0.01$), and * ($p < 0.001$)].**

evident in a co-occurrence network analysis, showing lower topology parameters, e.g. nodes, edges, and average path length in the intestinal microbial community of RP-treated caterpillars (Figure S7c and Table S3). Conversely, spatial variables primarily influence the *H. armigera* gut microbiome with HC. This gut microbiome was largely shaped by its host and exhibited more specific bacterial complexity and stable microbial structures. As for the dispersal mechanisms, neutral community models (NCM) show that the assembly of the phyllosphere and rhizosphere soil microbial community was primarily driven by stochastic processes (R^2 = 0.79 and R^2 = 0.77, Figure S8). However, in the presence of microbial diffusion in the phyllosphere, the intestinal microorganisms of *H. armigera* were enhanced by deterministic processes with a lower immigration rate (m = 0.02 explained by NCM). The nondominated process accounted for a greater proportion of control group's phyllosphere, while CBNP application enhanced the selection effect. With CBNP exposure, variable selection explained the phyllosphere bacterial community assembly across treatments. The higher absolute magnitude of standardized effect size for RP and HC treatment groups also indicates an increase in the relative contribution of deterministic processes (Figure S8d–f). It is worth noting that the two treatment groups exhibited distinct co-occurrence patterns of aggregation and segregation, demonstrating a differential influence of deterministic processes on the observed outcome (Figure S8g). Our results highlight the importance of determinism in shaping the community of CBNP-exposed groups by influencing niche selection and dispersal limitations, thereby explaining observed differences in the *H. armigera* gut microbial community structure and rhizosphere soil.

Pathway Dependency of Host-Microbiota Interplay Across Trophic Levels. Partial least-squares path models (PLS–PMs) account for 64% of the variance in the phyllosphere OTU shift (Figure 5), revealing a significant negative effect of CBNPs on phyllosphere OTUs (path coefficients: −0.80, $p < 0.01$). This confirms that CBNP suppressed shared OTUs across different habitats. To identify key microbial species involved in metastasis and CBNP transport, spearman correlation analysis was conducted to examine the interconnections between microbes and shift processes (Figure 5e). The results reveal strong associations between specific taxa (i.e., *Actinobacteriota, Bacteroidota, Patescibacteria*, and *Proteobacteria*) and microbial dispersal to rhizosphere soil. Moreover, *Planctomycetota* influenced the

https://doi.org/10.1021/acsnano.4c06047
ACS Nano 2024, 18, 25552–25564

effects of host-microbiota across trophic levels. Recent work has shown that *Planctomycetota* can have negative effects on organism survival and gut health.[57] This supports our hypothesis that CBNPs impact the interplay between host and associated microbiota across different trophic levels. Furthermore, dominant microbial communities within the phyllosphere may positively affect the translocation processes of CBNPs, particularly stem-to-root transfer within plants ($p < 0.01$). This further underscores the crucial role of microorganisms in the CBNP impact and transfer processes.

Exposure of cherry radish leaves to CBNPs could indirectly impact herbivore gut microbes through two pathways: (1) disrupted phyllosphere microbes may establish a symbiotic relationship within herbivores through host-microbiota transmission;[58] (2) the microbiome has a demonstrated ability to influence host plant metabolic processes, potentially affecting the microbiome of consumer species. Following an examination of host-microbiota transmission, we further integrated the analysis of phyllosphere microbes and leaf metabolic profiles to probe secondary bottom-up regulation pathways of plants on herbivores. The procrustes test suggests that alterations in the phyllosphere microbial community were likely associated with the perturbations in the metabolic profiles of plant leaves as a function of CBNP exposure ($M^2 = 0.353$, $p < 0.001$) (Figure S9). When focusing on the RP treatment, the reshaped *Pedobacter* and *Bosea* phyllosphere microbiome exhibited a strong correlation with various classes of differential metabolites (Figure S10). The plant growth-promoting bacteria *Bacillus* and *Pseudomonas* in HC treatments played a more significant role in regulating plant metabolism and thereby promoting host health by improving nutrient availability and accumulation.[59] This effect is evident in the observed increase in protein and flavonoid contents with HC exposure. There were 178 and 242 significantly changed metabolites (SCMs) in RP and HC treatments compared to control, respectively. The SCMs mainly included lipids and lipid-like molecules (fatty acyls and glycerophospholipids), phenylpropanoids and polyketides (flavonoids), organoheterocyclic compounds, benzenoids, organic acids and derivatives (amino acids, peptides, and analogues) and others (Figure S11). After RP exposure, there was significant enrichment in the KEGG pathway related to pyrimidine metabolism, pantothenate and CoA biosynthesis, and purine metabolic pathways (Figure S12). Compared with controls, ten pathways were significantly affected in the HC treatments, including aminoacyl-tRNA biosynthesis; phenylalanine biosynthesis; tyrosine and tryptophan biosynthesis; arginine and proline metabolism; pyrimidine metabolism; vitamin B6 metabolism; and purine, starch, and sucrose metabolism (Figure S12). These results suggest that CBNPs mainly influence the biosynthesis and metabolism of sugars and amino acids in cherry radish leaves, with HC having a more pronounced impact. Phenylalanine, tryptophan, arginine, and other essential amino acids necessary for insect growth have been identified as important taste recognition factors in the host selection process of herbivores.[60] The significantly up-regulated amino acid content in the leaves of the HC-exposed groups further explains the higher ingestion rate of *H. armigera* compared to the RP group. This regulatory impact was also confirmed by Mantel analysis, which demonstrated that the physicochemical properties and nutritional quality of cherry radish were directly or indirectly influenced by phyllosphere microbes and metabolites (Figure 6a–b). The interplay between phyllosphere microbes and metabolites emerges as a critical determinant of plant health and development. Notably, yield, and the vitamin and flavonoid content of cherry radish exhibited a meaningful correlation with *H. armigera* gut microbes (RC: $p < 0.05$; HC: $p < 0.01$). Moreover, leaf metabolites were found to exert a substantial influence on *H. armigera* grazing behavior and weight. These findings underscore a significant nexus between nutrient levels and the cascading effects mediated by CBNPs. Nanopesticides-induced copper homeostasis can enhance leaf quality by altering primary metabolism, while also indirectly supplying essential micronutrients to caterpillars, consequently influencing invertebrate phenotype. The pathway underlying bottom-up regulation of plants was quantitively evaluated by a conceptual framework (Figure 6c). In this framework, phyllosphere microbes were noted to positively contribute (path coefficients: 0.96, $p < 0.05$) to CBNPs trophic transfer, while concurrently exerting a negative influence (path coefficients: −1.12, $p < 0.05$) through metabolite alterations, ultimately affecting the ingestion of contaminated leaves by *H. armigera*. Beyond that, the gut microbial dysbiosis in *H. armigera* caused by CBNP-contaminated leaves is intricately linked to the physiological function of the host. *Bacteroidota* play a crucial role in enhancing mucosal tolerance and nutrient uptake by secreting anti-inflammatory cytokines and transforming indigestible carbohydrates.[61] Therefore, an increase in the relative abundance of *Bacteroidota* caused by ingestion of contaminated leaves promoted resistance to external stresses in *H. armigera*. Additionally, *Proteobacteria* is an essential group involved in nutrient recycling and is important to animal growth. The higher abundance of *Proteobacteria* induced better growth performance in RP *H. armigera* (Figure 2). Given that many gut microbes act as beneficial symbionts interacting with gut tissue, these species wield influence over host metabolism and overall health.[62] The functional prediction by PICRUSt analysis also indicated a relatively high abundance of gut bacterial functions associated with to carbohydrate and amino acid metabolism, which exhibited significant differences between treatment groups (Figure S13). This suggests their potential involvement in substance metabolism, as CBNPs impact the energy supply of *H. armigera* gut microbiota, thereby influencing host health. In summary, CBNPs perturbed both the microbiota composition and metabolite profile of cherry radish leaves, subsequently affecting the microbial community in *H. armigera* and its phenotype. Although the true significance of these changes remains unknown, it is clear that CBNP exposure has significant implications for the host-microbiota interplay, with potential downstream consequences via the food chain.

CONCLUSION

Due to disparities in their physicochemical properties, such as variances in aggregation tendency, the two types of CBNPs exhibit distinct levels of foliar enrichment and distribution patterns within the leaf despite their similar morphology. RP with a smaller hydraulic diameter is more readily uptake by plant leaves and accumulates primarily in the cuticle. HC tends to accumulate predominantly in the cuticle layer and subsequently releases a higher amount of Cu^{2+} ions that are transported toward the spongy mesophyll. The morphological transformations resulting from differences in solubility further influence the translocation of CBNPs in planta. However, no significant discrepancies were observed regarding trophic transfer of both CBNPs; as trophic levels increase, differences

https://doi.org/10.1021/acsnano.4c06047
ACS Nano 2024, 18, 25552−25564

in CBNP accumulation become less pronounced. This study also demonstrates the transmission of host-microbiota during CBNP trophic transfer, as well as the resulting impacts on host health, encompassing both the phyllosphere and the gut of *H. armigera*. The altered copper homeostasis induced by CBNPs may help maintain host health by recruiting beneficial microbes into the phyllosphere, mitigating stress, and altering metabolic pathways that improve plant quality. Furthermore, the transmission of host-microbiota induced by CBNP trophic transfer could serve as an effective strategy for introducing transient microbes into distinct microenvironments. The dispersal of phyllosphere microbes such as *Proteobacteria*, *Bacteroidota*, and *Actinobacteriota* directly influences the health and intestinal immunity of *H. armigera*. RP exhibits enhanced antibacterial effects, facilitating the spread of beneficial microbiota (*Bacteroidota*) from the phyllosphere to the *H. armigera* gut. This augmentation strengthens the resistance of caterpillars against environmental stress and exerts more pronounced regulatory effects on the host health. This bottom-up control effect is also contingent upon the regulation of molecular-level metabolite modifications in plants to *H. armigera* feeding behavior. By constructing a conceptual model, we quantitatively evaluated the possible pathways for bottom-up control, thereby contributing complementary insights into understanding the mechanisms of host-microbiota interplay on various trophic levels. This understanding can be instrumental in the development of strategies to mitigate negative impacts of nanopesticide on ecological services. Although the effects on the gut microbes of *H. armigera* by grazing Cu-containing leaves has been demonstrated, quantification of direct effects due to Cu transfer and indirect carried effects through predation remain somewhat undefined. Moreover, it is essential to consider the dynamic transformation processes of CBNPs while constructing a comprehensive ecological modeling framework; this will help identify the specific forms of copper involved in host-microbiota transmission. Further research is still necessary to incorporate the host-selective role of herbivores into dynamic modeling, and ultimately determine the correlation with whole-ecosystem level effects over time.

MATERIALS AND METHODS

Soils and Chemicals. The soil used in this study was collected from the plough layer (0−20 cm) of agricultural land located in Yingtan, Jiangxi, China (N28°15′20″, E116°55′30″). Details on the soil pretreatment and soil properties can be found in the Supporting Information (Text S1 and Table S1).

Following preliminary market research, two commercial $Cu(OH)_2$ products that are commonly available in the Chinese market were chosen for this study. The first product, Reap2000 [RP, 77% (p/p) $Cu(OH)_2$ and 23% dispersing agent (sodium salt of polynaphthalene sulfonic acid), powder], was purchased from the Zhejiang Ruili Biotechnology Co., Ltd. The second product, HolyCu (HC, 98.6% (p/p) $Cu(OH)_2$ with trace amounts of lauryl sodium sulfate and other elements, powder), was obtained from the Beijing Zhongke Leiming Technology Co., Ltd. The morphology of RP and HC was examined by transmission electron microscopy (TEM, Tecani G2 Spirit TWIN, Thermo Fisher Scientific, USA). The dissolution profile of the $Cu(OH)_2$ products was investigated and is described in Text S2.

Foliar and Trophic Exposure. The test plant chosen for this study was cherry radish (*Raphanus sativus* L.), a commonly consumed vegetable by humans, characterized by leaf stomatal areas larger than 30 μm^2, thereby facilitating an increased likelihood of entry for CBNPs. Cherry radish seeds (China Vegetable Seed Technology Co., Ltd.) were surface sterilized with 10% H_2O_2 and then germinated at 25 °C in the dark for 2 days. Four similar-sized seedlings were transplanted into a 1-gallon plastic pot filled with 1.2 kg experimental soil. Each treatment had four replicates. The cultures were randomly distributed in a climate chamber with a light/dark cycle of 16/8 h at 25 °C and 60% humidity. The soil water content was maintained at 60% of its maximum water-holding capacity by watering the pots to a constant weight every 2 days. Three weeks after cultivation, the radish plants were foliar sprayed with either of the CBNPs for 7 days considering the short planting cycle of cherry radish and the timing of metabolic reactions. Following the manufacturer's instructions, 1.5 mL of RP or HC suspensions [1000 mg/L for RP and HC, calculated based on the active ingredient nano-$Cu(OH)_2$] were sprayed four rounds, once every 2 days, totaling an amount of 6.0 mg of nano-$Cu(OH)_2$ per plant. Control groups consisted of radish plants sprayed with deionized water. Additional details on the foliar operation can be found in Text S3. At maturity (35 days), plants were harvested and relevant phenotypic indices were recorded. Samples of leaves, stems, and roots were washed with deionized water to remove any adhered particulates and CBNPs before further elemental, physiological and biochemical indicator analysis (Text S4). Some leaves underwent vacuum packing and storage at 4 °C for subsequent trophic exposure studies.

Caterpillars (*H. armigera*), a globally distributed polyphagous pest, cause significant economic losses to various crops. They are particularly problematic as the primary pests of cherry radish, hold crucial ecological importance, and their response to CBNPs can serve as an indicator of potential risks to the environment and human health. They were ordered from Keyun Biotechnology Co., Ltd. (Henan, China) and sorted into culture dishes (90 mm × 90 mm × 15 mm). Each replication consisted of ten individuals, and each treatment was replicated four times. Healthy and active second-instar larvae weighing approximately 0.01 g were selected as test animals and were depurated before the exposure experiments. The leaves exposed to CBNPs were provided as a diet at a rate of 0.4 g/day per caterpillar. During a one-week exposure period, the weight and daily consumption of leaves by all caterpillars were monitored closely, and any unconsumed leaves were removed before the next round of feeding commenced. At predefined time points (0, 1, 2, 4, and 7 days), feces were collected. Harvested caterpillars were depurated for 24 h before being frozen in liquid nitrogen and stored at −80 °C for elemental analysis.

Elemental Analysis of Cherry Radish, Caterpillar and Soil. Collected cherry radish leaves were divided into three fractions: the surface wash fraction, cuticle fraction, and interior leaf fraction. For detailed separation steps, see Supporting Information Text S5. The samples of interior leaves (both rinsed and decuticled), shoots, roots, caterpillars and their feces underwent drying prior to digestion in a graphite biogas digester with HNO_3. Soil samples were collected, air-dried, sieved through a 100 mesh, and digested using an automatic microwave system with $HCl-HNO_3-H_2O_2$ (Topwave, Analytic Jena, Germany). The content of Cu and other nutrient elements in plants, caterpillars, feces, and soil samples were analyzed by inductively coupled plasma mass spectrometry (ICP−MS, iCAP-Q, Thermo Fisher, America). Meanwhile, reference soil material (GBW07405) and biological materials (GBW07603) were used as quality control/quality assurance measures. Specifics regarding recovery rates are described in Table S2.

DNA Extraction and Sequencing. Rhizosphere soil samples were collected according to Riley et al.[63] Soil DNA was isolated from 0.5 g of rhizosphere soil per replicate using a FastDNA Spin Kit for Soil (MP Biomedicals, USA). For the extraction of phyllosphere microbe DNA, the procedure of Zheng et al.[64] was followed. Approximately 5 g fresh leaves per replicate was weighed and washed with 100 mL of 0.01 M sterile PBS containing 0.02% Tween 20. After ultrasound treatment and incubation, the buffer solution was filtered through a 0.22 μm filter membrane for subsequent DNA extraction using a FastDNASpin Kit. To obtain caterpillar gut DNA, the animal was surface sterilized by soaking in 70% ethyl alcohol for 30 s, followed by a 1 min immersion in 0.25% sodium hypochlorite solution. After rinsing thrice with sterile water to eliminate external

https://doi.org/10.1021/acsnano.4c06047
ACS Nano 2024, 18, 25552−25564

contaminants, gut dissection was performed using sterile needles and forceps. Total gut DNA was extracted from 10 caterpillars as a replicate using a FastDNASpin Kit according to the manufacturer's instructions. The details of PCR amplification and sequencing are described in Text S6.

Metabolomic Analysis. After exposure, leaf metabolites were extracted by vortexing in a mixture of methanol/acetonitrile/water (2:2:1, v/v). The extracts were then sonicated at low temperature (0−4 °C) for 30 min and centrifuged for 20 min (14,000*g*, 4 °C). The resulting supernatant was vacuum-dried and stored at −80 °C. Prior to testing, a solution of acetonitrile and water (1:1, v/v) was added for redissolution. An ultrahigh-performance liquid chromatography (UHPLC) system (1290 Infinity LC, Agilent Technologies, USA) equipped with an ACQUITY BEH C18 column (100 mm × 2.1 mm i.d., 1.7 μm; Waters, Milford, USA) was used for chromatographic separation of cherry radish leaf metabolites. The mass spectrometric data was collected using a UHPLC-Q Exactive Mass Spectrometer coupled with an electrospray ionization source operating in positive or negative ion mode.

Statistical Analysis. All experimental data except metabolomic and microbe data were reported as average values ±standard deviation (n = 4). An unpaired Student's t-test on single-dimensional statistical analysis using GraphPad Prism (version 9.0) was employed to detect significant differences between treatments for element concentrations, oxidative stress levels, antioxidative systems, and nutritional quality. PLS−PMs, constructed by the "plspm" package in R4.2.3, were used to identify the coordinating role of phyllosphere microorganisms for bottom-up control. Detailed information on the data analysis of trophic transfer and toxicokinetic model construction is described in Text S7. Additional details on the bioinformatics analysis of metabolomics and microbiome data can be found in Text S8.

ASSOCIATED CONTENT

Supporting Information

The Supporting Information is available free of charge at https://pubs.acs.org/doi/10.1021/acsnano.4c06047.

The Supporting Information contains: Supplementary methods, soil sampling and pretreatment, dissolved Cu release from CBNPs, the foliar application method, cuticle Cu extraction, determination of physiological and biochemical indicators, calculation of CBNP translocation and trophic transfer, 16S rRNA gene amplicon sequencing and detailed bioinformatics analysis (PDF)

AUTHOR INFORMATION

Corresponding Author

Hao Qiu − *School of Environmental Science and Engineering, Shanghai Jiao Tong University, Shanghai 200240, China;* orcid.org/0000-0002-4743-9702; Email: haoqiu@sjtu.edu.cn

Authors

Xuchen Yan − *School of Environmental Science and Engineering, Shanghai Jiao Tong University, Shanghai 200240, China*

Jason C. White − *The Connecticut Agricultural Experiment Station, New Haven 06511 Connecticut, United States;* orcid.org/0000-0001-5001-8143

Erkai He − *School of Geographic Sciences, East China Normal University, Shanghai 200241, China;* orcid.org/0000-0002-4866-3001

Willie J.G.M. Peijnenburg − *Center for the Safety of Substances and Products, National Institute of Public Health and the Environment, Bilthoven 3720BA, The Netherlands; Institute of Environmental Sciences, Leiden University, Leiden 2300RA, The Netherlands;* orcid.org/0000-0003-2958-9149

Peng Zhang − *School of Geography, Earth and Environmental Sciences, University of Birmingham, Edgbaston B15 2TT Birmingham, U.K.;* orcid.org/0000-0002-2774-5534

Complete contact information is available at: https://pubs.acs.org/10.1021/acsnano.4c06047

Notes

The authors declare no competing financial interest.

ACKNOWLEDGMENTS

This study was supported by the National Natural Science Foundation of China (nos. 42377268, 42277117) and the National Key Research & Development Program of China (no. 2023YFC3711500).

REFERENCES

(1) Zhao, L.; Ortiz, C.; Adeleye, A. S.; Hu, Q.; Zhou, H.; Huang, Y.; Keller, A. A. Metabolomics to detect response of lettuce (*Lactuca sativa*) to $Cu(OH)_2$ nanopesticides: oxidative stress response and detoxification mechanisms. *Environ. Sci. Technol.* **2016**, *50* (17), 9697−9707.

(2) Liu, P.; Yang, M.; Hermanowicz, S. W.; Huang, Y. Efficacy-associated cost analysis of copper-based nanopesticides for tomato disease control. *ACS Agric. Sci. Technol.* **2022**, *2* (4), 796−804.

(3) Kah, M.; Tufenkji, N.; White, J. C. Nano-enabled strategies to enhance crop nutrition and protection. *Nat. Nanotechnol.* **2019**, *14* (6), 532−540.

(4) Hong, J.; Wang, C.; Wagner, D. C.; Gardea-Torresdey, J. L.; He, F.; Rico, C. M. Foliar application of nanoparticles: mechanisms of absorption, transfer, and multiple impacts. *Environ. Sci. Nano* **2021**, *8* (5), 1196−1210.

(5) Patel, P.; Kumar Jatav, P.; Jain, R.; Gupta, S.; Kothari, S. L.; Kachhwaha, S. Humidity induced opening of stomata leads to enhanced uptake of copper nanoparticles in *Triticum aestivum* L. *Mater. Today: Proc.* **2021**, *43* (5), 3191−3196.

(6) El-Shetehy, M.; Moradi, A.; Maceroni, M.; Reinhardt, D.; Petri-Fink, A.; Rothen-Rutishauser, B.; Mauch, F.; Schwab, F. Silica nanoparticles enhance disease resistance in Arabidopsis plants. *Nat. Nanotechnol.* **2021**, *16* (3), 344−353.

(7) Shen, Y.; Borgatta, J.; Ma, C.; Elmer, W.; Hamers, R. J.; White, J. C. Copper nanomaterial morphology and composition control foliar transfer through the cuticle and mediate resistance to root fungal disease in tomato (*Solanum lycopersicum*). *J. Agric. Food Chem.* **2020**, *68* (41), 11327−11338.

(8) Su, Y.; Ashworth, V.; Kim, C.; Adeleye, A. S.; Rolshausen, P.; Roper, C.; White, J.; Jassby, D. Delivery, uptake, fate, and transport of engineered nanoparticles in plants: A critical review and data analysis. *Environ. Sci. Nano* **2019**, *6* (8), 2311−2331.

(9) Gall, J. E.; Boyd, R. S.; Rajakaruna, N. Transfer of heavy metals through terrestrial food webs: a review. *Environ. Monit. Assess.* **2015**, *187* (4), 201.

(10) Wu, J.; Sun, J.; Bosker, T.; Vijver, M. G.; Peijnenburg, W. J. G. M. Toxicokinetics and particle number-based trophic transfer of a metallic nanoparticle mixture in a terrestrial food chain. *Environ. Sci. Technol.* **2023**, *57* (7), 2792−2803.

(11) Wu, J.; Bosker, T.; Vijver, M. G.; Peijnenburg, W. J. G. M. Trophic transfer and toxicity of (mixtures of) Ag and TiO_2 nanoparticles in the lettuce-terrestrial snail food chain. *Environ. Sci. Technol.* **2021**, *55* (24), 16563−16572.

(12) Li, J. R.; Rodrigues, S.; Tsyusko, O. V.; Unrine, J. M. Comparing plant-insect trophic transfer of Cu from lab-synthesised nano-$Cu(OH)_2$ with a commercial nano-$Cu(OH)_2$ fungicide formulation. *Environ. Chem.* **2019**, *16* (6), 411−418.

(13) Jager, T.; Albert, C.; Preuss, T. G.; Ashauer, R. General unified threshold model of survival - a toxicokinetic-toxicodynamic frame-

work for ecotoxicology. *Environ. Sci. Technol.* **2011**, *45* (7), 2529−2540.
(14) Steffan, S. A.; Dharampal, P. S. Undead food-webs: Integrating microbes into the food-chain. *Food Webs* **2019**, *18*, No. e00111.
(15) Thakur, M. P.; Geisen, S. Trophic Regulations of the Soil Microbiome. *Trends Microbiol.* **2019**, *27* (9), 771−780.
(16) Zhu, Y.-G.; Xiong, C.; Wei, Z.; Chen, Q.-L.; Ma, B.; Zhou, S.-Y.-D.; Tan, J.; Zhang, L.-M.; Cui, H.-L.; Duan, G.-L. Impacts of global change on the phyllosphere microbiome. *New Phytol.* **2022**, *234* (6), 1977−1986.
(17) Hussain, M.; Shakoor, N.; Adeel, M.; Ahmad, M. A.; Zhou, H.; Zhang, Z.; Xu, M.; Rui, Y.; White, J. C. Nano-enabled plant microbiome engineering for disease resistance. *Nano Today* **2023**, *48*, 101752.
(18) Ahmed, T.; Noman, M.; Gardea-Torresdey, J. L.; White, J. C.; Li, B. Dynamic interplay between nano-enabled agrochemicals and the plant-associated microbiome. *Trends Plant Sci.* **2023**, *28* (11), 1310−1325.
(19) Adomako, M. O.; Yu, F.-H. Potential effects of micro- and nanoplastics on phyllosphere microorganisms and their evolutionary and ecological responses. *Sci. Total Environ.* **2023**, *884*, 163760.
(20) Cao, W.; Gong, J.; Zeng, G.; Qin, M.; Qin, L.; Zhang, Y.; Fang, S.; Li, J.; Tang, S.; Chen, Z. Impacts of typical engineering nanomaterials on the response of rhizobacteria communities and rice (*Oryza sativa* L.) growths in waterlogged antimony-contaminated soils. *J. Hazard. Mater.* **2022**, *430*, 128385.
(21) Vorholt, J. A. Microbial life in the phyllosphere. *Nat. Rev. Microbiol.* **2012**, *10* (12), 828−840.
(22) Abdelfattah, A.; Wisniewski, M.; Schena, L.; Tack, A. J. M. Experimental evidence of microbial inheritance in plants and transmission routes from seed to phyllosphere and root. *Environ. Microbiol.* **2021**, *23* (4), 2199−2214.
(23) Liu, H. W.; Brettell, L. E.; Singh, B. Linking the phyllosphere microbiome to plant health. *Trends Plant Sci.* **2020**, *25* (9), 841−844.
(24) Abadi, V.; Sepehri, M.; Rahmani, H. A.; Dolatabad, H. K.; Shamshiripour, M.; Khatabi, B. Diversity and abundance of culturable nitrogen-fixing bacteria in the phyllosphere of maize. *J. Appl. Microbiol.* **2021**, *131* (2), 898−912.
(25) Xu, N.; Zhao, Q.; Zhang, Z.; Zhang, Q.; Wang, Y.; Qin, G.; Ke, M.; Qiu, D.; Peijnenburg, W. J. G. M.; Lu, T.; et al. Phyllosphere microorganisms: sources, drivers, and their interactions with plant hosts. *J. Agric. Food Chem.* **2022**, *70* (16), 4860−4870.
(26) Burgess, E. C.; Schaeffer, R. N. The floral microbiome and its management in agroecosystems: a perspective. *J. Agric. Food Chem.* **2022**, *70* (32), 9819−9825.
(27) Fang, B.; Li, J. W.; Zhang, M.; Ren, F. Z.; Pang, G. F. Chronic chlorpyrifos exposure elicits diet-specific effects on metabolism and the gut microbiome in rats. *Food Chem. Toxicol.* **2018**, *111*, 144−152.
(28) Gaulke, C. A.; Barton, C. L.; Proffitt, S.; Tanguay, R. L.; Sharpton, T. J. Triclosan exposure is associated with rapid restructuring of the microbiome in adult zebrafish. *PloS One* **2016**, *11* (5), No. e0154632.
(29) Li, G.; Yin, B.; Li, J.; Wang, J.; Wei, W.; Bolnick, D. I.; Wan, X.; Zhu, B.; Zhang, Z. Host-microbiota interaction helps to explain the bottom-up effects of climate change on a small rodent species. *ISME J.* **2020**, *14* (7), 1795−1808.
(30) Chen, T.; Nomura, K.; Wang, X. L.; Sohrabi, R.; Xu, J.; Yao, L. Y.; Paasch, B. C.; Ma, L.; Kremer, J.; Cheng, Y. T.; et al. A plant genetic network for preventing dysbiosis in the phyllosphere. *Nature* **2020**, *580* (7805), 653−657.
(31) Raza, M. A. S.; Amin, J.; Valipour, M.; Iqbal, R.; Aslam, M. U.; Zulfiqar, B.; Muhammad, F.; Ibrahim, M. A.; Al-Ghamdi, A. A.; Elshikh, M. S.; et al. Cu-nanoparticles enhance the sustainable growth and yield of drought-subjected wheat through physiological progress. *Sci. Rep-UK.* **2024**, *14*, 14254.
(32) Abdel-Ghany, S. E.; Muller-Moule, P.; Niyogi, K. K.; Pilon, M.; Shikanai, T. Two P-type ATPases are required for copper delivery in Arabidopsis thaliana chloroplasts. *Plant Cell* **2005**, *17*, 1233−1251.
(33) Fedorov, V. A.; Kovalenko, I. B.; Khruschev, S. S.; Ustinin, D. M.; Antal, T. K.; Riznichenko, G. Y.; Rubin, A. B. Comparative analysis of plastocyanin-cytochrome f complex formation in higher plants, green algae and cyanobacteria. *Plant Physiol.* **2019**, *166*, 320−335.
(34) Tan, W.; Gao, Q.; Deng, C.; Wang, Y.; Lee, W.-Y.; Hernandez-Viezcas, J. A.; Peralta-Videa, J. R.; Gardea-Torresdey, J. L. Foliar exposure of $Cu(OH)_2$ nanopesticide to basil (*Ocimum basilicum*): Variety-dependent copper translocation and biochemical responses. *J. Agric. Food Chem.* **2018**, *66* (13), 3358−3366.
(35) Chen, G.; Li, J.; Han, H.; Du, R.; Wang, X. Physiological and molecular mechanisms of plant responses to copper stress. *Int. J. Mol. Sci.* **2022**, *23* (21), 12950.
(36) Li, S.; Liu, J.; Wang, Y.; Gao, Y.; Zhang, Z.; Xu, J.; Xing, G. Comparative physiological and metabolomic analyses revealed that foliar spraying with zinc oxide and silica nanoparticles modulates metabolite profiles in cucumber (*Cucumis sativus* L.). *Food Energy Secur.* **2021**, *10* (1), No. e269.
(37) Hu, J.; Guo, H.; Li, J.; Wang, Y.; Xiao, L.; Xing, B. Interaction of γ-Fe_2O_3 nanoparticles with Citrus maxima leaves and the corresponding physiological effects via foliar application. *J. Nanobiotechnol.* **2017**, *15* (1), 51.
(38) Lian, J.; Zhao, L.; Wu, J.; Xiong, H.; Bao, Y.; Zeb, A.; Tang, J.; Liu, W. Foliar spray of TiO_2 nanoparticles prevails over root application in reducing Cd accumulation and mitigating Cd-induced phytotoxicity in maize (*Zea mays* L.). *Chemosphere* **2020**, *239*, 124794.
(39) Gill, S. S.; Tuteja, N. Reactive oxygen species and antioxidant machinery in abiotic stress tolerance in crop plants. *Plant Physiol. Biochem.* **2010**, *48*, 909−930.
(40) Hernández, I.; Alegre, L.; Van Breusegem, F.; Munné-Bosch, S.; et al. How relevant are flavonoids as antioxidants in plants? *Trends Plant Sci.* **2009**, *14*, 125−132.
(41) Avellan, A.; Yun, J.; Zhang, Y. L.; Spielman-Sun, E.; Unrine, J. M.; Thieme, J.; Li, J. R.; Lombi, E.; Bland, G.; Lowry, G. V. Nanoparticle size and coating chemistry control foliar uptake pathways, translocation, and leaf-to-rhizosphere transport in wheat. *ACS Nano* **2019**, *13* (5), 5291−5305.
(42) Ouyang, X.; Ma, J.; Zhang, R.; Li, P.; Gao, M.; Sun, C.; Weng, L.; Chen, Y.; Yan, S.; Li, Y. Uptake of atmospherically deposited cadmium by leaves of vegetables: Subcellular localization by NanoSIMS and potential risks. *J. Hazard. Mater.* **2022**, *431*, 128624.
(43) Larue, C.; Castillo-Michel, H.; Sobanska, S.; Trcera, N.; Sorieul, S.; Cécillon, L.; Ouerdane, L.; Legros, S.; Sarret, G. Fate of pristine TiO_2 nanoparticles and aged paint-containing TiO_2 nanoparticles in lettuce crop after foliar exposure. *J. Hazard. Mater.* **2014**, *273*, 17−26.
(44) Gao, X. Y.; Kundu, A.; Persson, D. P.; Szameitat, A.; Minutello, F.; Husted, S.; Ghoshal, S. Application of ZnO Nanoparticles Encapsulated in Mesoporous Silica on the Abaxial Side of a *Solanum lycopersicum* Leaf Enhances Zn Uptake and Translocation via the Phloem. *Environ. Sci. Technol.* **2023**, *57* (51), 21704−21714.
(45) Zhang, P. J.; Wang, K. L.; He, L. F.; Fan, R. J.; Liu, Z. F.; Yang, J.; Guo, R. F.; Gao, Y. Surfactants improving the wetting behavior and adhesion mechanism of pesticide dilution droplets on jujube leaf surfaces. *ACS Omega* **2023**, *8* (24), 22121−22131.
(46) Morgado, R. G.; Pavlaki, M. D.; Soares, A.; Loureiro, S. Terrestrial organisms react differently to nano and non-nano $Cu(OH)_2$ forms. *Sci. Total Environ.* **2022**, *807*, 150679.
(47) Amyot, M.; Clayden, M. G.; MacMillan, G. A.; Perron, T.; Arscott-Gauvin, A. Fate and trophic transfer of rare earth elements in temperate lake food webs. *Environ. Sci. Technol.* **2017**, *51* (11), 6009−6017.
(48) Ma, Y.; Yao, Y.; Yang, J.; He, X.; Ding, Y.; Zhang, P.; Zhang, J.; Wang, G.; Xie, C.; Luo, W.; et al. Trophic transfer and transformation of CeO_2 nanoparticles along a terrestrial food chain: influence of exposure routes. *Environ. Sci. Technol.* **2018**, *52* (14), 7921−7927.
(49) Kubo-Irie, M.; Yokoyama, M.; Shinkai, Y.; Niki, R.; Takeda, K.; Irie, M. The transfer of titanium dioxide nanoparticles from the host

plant to butterfly larvae through a food chain. *Sci. Rep-UK.* **2016**, *6* (1), 23819.
(50) Liu, M.; Korpelainen, H.; Li, C. Y. Sexual differences and sex ratios of dioecious plants under stressful environments. *J. Plant Ecol.* **2021**, *14* (5), 920−933.
(51) Xu, H.; Zhang, P. H.; He, E. R.; Peijnenburg, W. J. G. M.; Cao, X. D.; Zhao, L.; Xu, X. Y.; Qiu, H. Natural formation of copper sulfide nanoparticles via microbially mediated organic sulfur mineralization in soil: Processes and mechanisms. *Geoderma* **2023**, *430*, 116300.
(52) Shi, R.; Liu, W.; Lian, Y.; Wang, X.; Men, S.; Zeb, A.; Wang, Q.; Wang, J.; Li, J.; Zheng, Z.; et al. Toxicity mechanisms of nanoplastics on crop growth, interference of phyllosphere microbes, and evidence for foliar penetration and translocation. *Environ. Sci. Technol.* **2024**, *58* (2), 1010−1021.
(53) Qiao, R. X.; Deng, Y. F.; Zhang, S. H.; Wolosker, M. B.; Zhu, Q. D.; Ren, H. Q.; Zhang, Y. Accumulation of different shapes of microplastics initiates intestinal injury and gut microbiota dysbiosis in the gut of zebrafish. *Chemosphere* **2019**, *236*, 124334.
(54) Zhang, J.; Xia, X. H.; Ma, C. X.; Zhang, S. W.; Li, K. X.; Yang, Y. Y.; Yang, Z. F. Nanoplastics affect the bioaccumulation and gut toxicity of emerging perfluoroalkyl acid alternatives to aquatic insects (*Chironomus kiinensis*): Importance of plastic surface charge. *ACS Nano* **2024**, *18* (7), 5752−5765.
(55) Lee, S. M.; Kong, H. G.; Song, G. C.; Ryu, C. M. Disruption of *Firmicutes* and *Actinobacteria* abundance in tomato rhizosphere causes the incidence of bacterial wilt disease. *ISME J.* **2021**, *15* (1), 330−347.
(56) Kachel, M.; Nowak, A.; Jaroszuk-Scisel, J.; Tyskiewicz, R.; Parafiniuk, S.; Rabier, F. Influence of Inorganic Metal (Ag, Cu) Nanoparticles on Biological Activity and Biochemical Properties of Brassica napus Rhizosphere Soil. *Agriculture-Basel* **2021**, *11* (12), 1215.
(57) Wang, M.; Fan, Z.; Zhang, Z.; Yi, M.; Liu, Z.; Ke, X.; Gao, F.; Cao, J.; Lu, M. Effects of diet on the gut microbial communities of Nile tilapia (*Oreochromis niloticus*) across their different life stages. *Front. Mar. Sci.* **2022**, *9*, 926132.
(58) Marchesi, J. R.; Adams, D. H.; Fava, F.; Hermes, G. D. A.; Hirschfield, G. M.; Hold, G.; Quraishi, M. N.; Kinross, J.; Smidt, H.; Tuohy, K. M.; et al. The gut microbiota and host health: a new clinical frontier. *Gut* **2016**, *65* (2), 330−339.
(59) Wang, C. A. X.; Yue, L.; Cheng, B. X.; Chen, F. R.; Zhao, X. L.; Wang, Z. Y.; Xing, B. S. Mechanisms of growth-promotion and Se-enrichment in*Brassica chinensis*L. by selenium nanomaterials: beneficial rhizosphere microorganisms, nutrient availability, and photosynthesis. *Environ. Sci. Nano* **2022**, *9* (1), 302−312.
(60) Wu, G. Y. Dietary requirements of synthesizable amino acids by animals: a paradigm shift in protein nutrition. *J. Anim. Sci. Biotechnol.* **2014**, *5* (1), 34.
(61) Zhang, X.; Wen, K.; Ding, D. X.; Liu, J. T.; Lei, Z.; Chen, X. X.; Ye, G. Z.; Zhang, J.; Shen, H. Q.; Yan, C. Z.; et al. Size-dependent adverse effects of microplastics on intestinal microbiota and metabolic homeostasis in the marine medaka (Oryzias melastigma). *Environ. Int.* **2021**, *151*, 106452.
(62) Daisley, B. A.; Chmiel, J. A.; Pitek, A. P.; Thompson, G. J.; Reid, G. Missing Microbes in Bees: How Systematic Depletion of Key Symbionts Erodes Immunity. *Trends Microbiol.* **2020**, *28* (12), 1010−1021.
(63) Riley, D.; Barber, S. A. Bicarbonate accumulation and pH changes at the soybean (*Glycine max* (L.) Merr.) root-soil interface. *Soil Sci. Soc. Am. J.* **1969**, *33* (6), 905−908.
(64) Zheng, F.; Zhou, G.-W.; Zhu, D.; Neilson, R.; Zhu, Y.-G.; Chen, B.; Yang, X.-R. Does plant identity affect the dispersal of resistomes above and below ground? *Environ. Sci. Technol.* **2022**, *56* (21), 14904−14912.

https://doi.org/10.1021/acsnano.4c06047
ACS Nano 2024, 18, 25552−25564